Glass forming banana-shaped compounds: Vitrified liquid crystal states

S. Rauch,[1] C. Selbmann,[1] P. Bault,[1] H. Sawade,[1] G. Heppke,[1] O. Morales-Saavedra,[2] M. Y. M. Huang,[3] and A. Jákli[3]
[1]*Technische Universität Berlin, Stranski-Laboratorium, Sekr. ER 11, Straße des 17 Juni 135, 10623 Berlin, Germany*
[2]*Technische Universität Berlin, Optisches Institut, Sekr. P1-1, Straße des 17 Juni 135, 10623 Berlin, Germany*
[3]*Liquid Crystal Institute, Kent State University, Kent, Ohio 44242, USA*
(Received 3 December 2002; published 27 February 2004)

The synthesis and physical properties, in particular electro-optic switching behavior, of 3-chloro-biphenyl-3′,4-bis{4-[4-(3,7-dimethyloctyloxy)-phenyliminomethyl]} benzoate are reported. The compound exhibits an antiferroelectric tilted smectic liquid crystalline phase (Sm-CP) in a broad temperature range. Below 20 °C the sample goes over to a glassy state and no crystallization appeares down to −50 °C. It is observed that below the glass transition temperature both achiral and chiral structures of the Sm-CP phase can be frozen. Each of them can have three polarization states (two ferroelectric and one antiferroelectric), thus giving six different vitrified textures. This enables atomic force microscopy studies of the different liquid crystalline states and suggests possibilities for electro-optical storage devices.

DOI: 10.1103/PhysRevE.69.021707 PACS number(s): 61.30.Eb, 61.30.Cz, 61.30.Gd

I. INTRODUCTION

Bent (banana-shaped) molecules have become a main topic of liquid crystal research since the first observation of ferroelectric properties in a series of homologous compounds by Niori *et al.* [1]. Although the molecules are achiral, the liquid crystalline phases formed by these materials have chiral properties. According to Link *et al.* [2], the combination of molecular tilt and polar in-layer ordering leads to chiral layers, which may be stacked to give either achiral or chiral domains. Most of the tilted polar (Sm-CP) phases show antiferroelectric-type switching [3], although recently some ferroelectric ground states have also been observed [4–6]. Above a threshold field ($E_{th}\sim 3-6\ \mathrm{V}/\mu\mathrm{m}$), the antiferroelectric ground states can be switched to ferroelectric. During the switching the layer chirality tends to be conserved [2], but recently it was found that the overall chiral character of the domains can also be gradually interchanged by application of suitable electric fields [7,8].

Typically, the banana smectic phases are at elevated temperatures, which makes their study more difficult and also reduces their stability. Therefore, for both practical and scientific reasons, it is desirable to have broad and room temperature range smectic phases. To our best knowledge so far only mixtures have showed room temperature switching [9,10]. In the present paper we report the synthesis and physical properties of a banana-shaped compound that not only possesses a mesophase in a broad temperature range including room temperature, but also forms a glassy state instead of crystallizing. This means that one can freeze mesophase structures, which would allow their detailed investigation by surface imaging, like atomic force microscopy, as was demonstrated recently on quenched cells [11]. In fact, we will show that one can freeze six different liquid crystalline structures, which implies their potential use in electro-optical storage devices.

II. EXPERIMENTAL SECTION

A. Materials

Detailed analysis of the phase behavior of several known [3] and recently synthesized compounds [12] indicated that a chlorine substituent in position 4 of the central biphenyl or phenyl core not only suppresses the clearing temperature but also leads to a broadening of the phase range. In addition, the tendency to form the crystalline state is reduced by introduction of a bulkier terminal chain, represented here by use of (rac)-3,7-dimethyloctanol as precursor.

As shown in Fig. 1, 3-methoxybenzene boronic acid and 4-bromo-1-butoxy-2-chloro-benzene were refluxed for 4 h in a mixture of benzene and aqueous sodium carbonate solution in the presence of palladium tetrakis triphenyl phosphine (the Suzuki cross coupling reaction) to give 4-butoxy-3-chloro-3′-methoxy-biphenyl after purification by column chromatography (hexane:methylene chloride, 9:1, v:v). Cleavage of ethers using boron tribromide in methylene chloride gave the corresponding diol [Fig. 1(c)]. Esterification of the diol with 4-carboxybenzaldehyde was performed in methylene chloride using the classical n,n'-dicyclohexylcarbodiimide-4-dimethylaminopyridine (DCC-DMAP) method to give the structure in Fig. 1(d) after crystallization from ethanol.

The product Fig. 1(g) was achieved in two steps: first by a Mitsunobu reaction between 4-acetamidophenol and (R/S)-3-7-dimethyloctanol, followed by deacetalyzation with potassium hydroxide by refluxing in ethanol for 6 h.

The Schiff base (R/S)-BiPhe [13] was prepared by standard condensation between the dialdehyde [Fig. 1(d)] and two equivalents of aminoether [Fig. 1(g)] in the presence of a catalytic amount of acetic acid. The precipitate was purified by several recrystallizations from ethanol before using for physical investigations.

B. Phase characterization

The biphenyl compound given in Fig. 1, composed of four stereoisomers, shows one broad liquid crystalline phase range without crystallization down to −50 °C (see Fig. 2).

Polarizing microscopic investigations on thin samples sandwiched between two glass plates show that the smectic phase grows from the isotropic liquid in the form of porridgelike textures typical for banana-shaped compounds with direct isotropic to Sm-CP phase transitions (see Fig. 3). Small striped fans with different birefringences are formed.

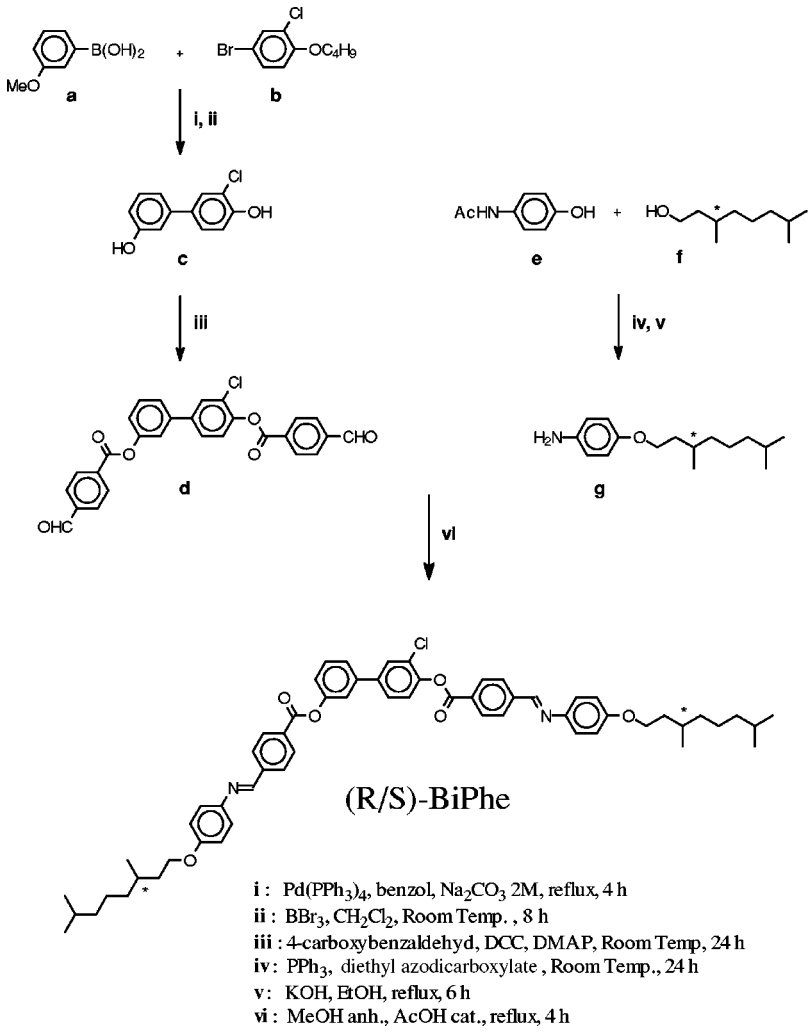

FIG. 1. Synthetic pathway of 3-chloro-biphenyl-3′,4-bis{4-[4-(3,7-dimethyl-octyloxy)-phenyliminomethyl]} benzoate, designated as (R/S)-BiPhe.

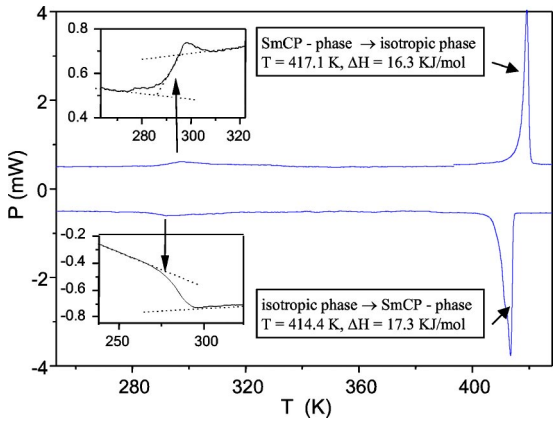

FIG. 2. Differential scanning calorigram as measured in heating (upper curve) and cooling. Below the isotropic to Sm-*CP* phase transition ($T_i = 417.1$ K, measured in heating at a rate of 3 K/min), there is no sign of crystallization. At around 290 K a stepwise change of slope indicates a glass transition. Note that the curves are baseline corrected for graphical representation.

In some areas dark regions with grayish schlieren textures indicate that there the molecular long axis connecting the end points of the bisubstituted biphenyl core is almost normal to the glass substrate. The phase assignment has been confirmed by miscibility studies with the standard compounds 8-PIMB [1] and 14-PIMB [8] (1,3-phenylinebis[4-(4-n-alkylphenyliminomethyl)benzoates]).

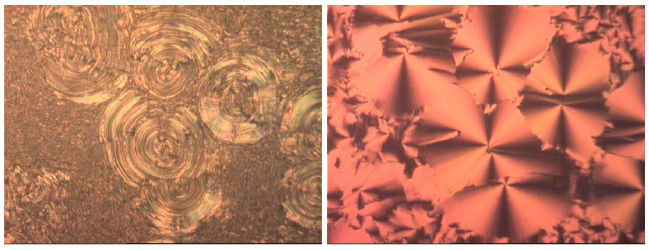

FIG. 3. Polarizing micrographs of (R/S)-BiPhe at $T = 123\,^{\circ}$C in a 10 μm thick test cell (from E.H.C. Co.) with parallel rubbed polyimide substrates, as observed coming from the isotropic phase at a cooling rate of 0.3 K/min under application of a bipolar square-wave electric field of $E = 6$ V/μm, $f = 1$ kHz. Texture at $E =$ (a) 0; (b) 15 V/μm bias fields. Texture does not depend on the sign of the electric field applied.

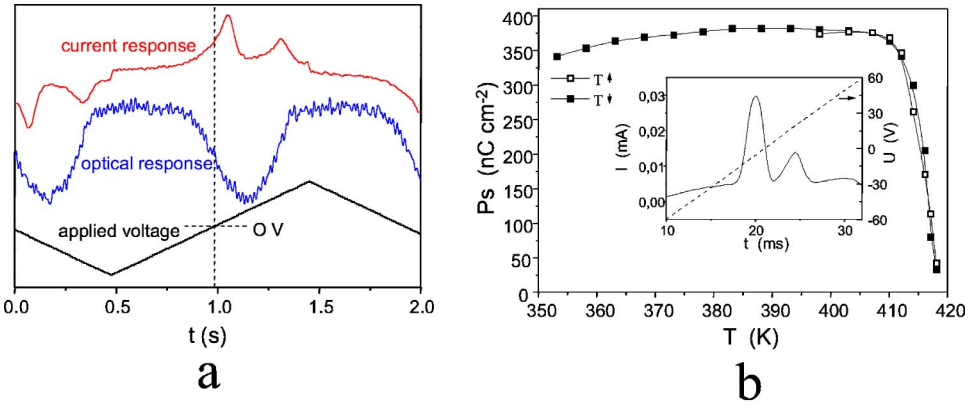

FIG. 4. (a) Electro-optical response of a $d=10\ \mu$m thick (R/S)-BiPhe film at $T=40\,^{\circ}$C under application of $f=0.5$ Hz, $E=15\ \mathrm{V}/\mu$m field; (b) temperature dependence of the spontaneous polarization measured in cooling.

C. Experimental results

Electro-optic and polarization current responses of a $d=10\ \mu$m thick test cell filled with (R/S)-BiPhe are shown in Fig. 4. Low frequency ($f<10$ Hz) triangular electric fields result in separate polarization peaks on both the negative and positive sides of the applied fields, and the optical response is insensitive to the sign of the electric field, indicating an achiral-type layer structure. At frequencies higher than 10 Hz, however, there is only one peak [see Fig. 5(a)]. It is interesting to note that at low frequencies and at high temperatures [see Fig. 5(b)] the peak appears in decreasing fields, whereas in ferroelectric Sm-C^* materials the switching usually occurs in increasing fields. Later, we will show that such polarization current curves can also appear in antiferroelectric materials, provided that the antiferroelectric order reforms only slowly and there are insulating alignment layers.

At low temperatures near the glass transition, the viscosity of the sample becomes so high that the polarization reversal peaks are broadened and are no longer visible. To study the kinetics at low temperatures, we measured the optical relaxation connected to the ferroelectric switching. Because it is difficult to achieve uniform alignment of banana-shaped smectics, we utilized the different scattering properties of the field-induced ferroelectric states when compared to the antiferroelectric ground states. As shown recently [10], the achiral antiferroelectric ground state (Sm-C_SP_A) is highly scattering, while the field-induced ferroelectric state (Sm-C_AP_F) is transparent. In the chiral state the situation is reversed: the ground state (Sm-C_AP_A) is transparent, whereas the field-induced ferroelectric state (Sm-C_SP_F) is opaque.

The time dependence of the transmission of white light in normal incidence was measured at different temperatures in a 4 μm test cell after removal of a dc bias voltage. The switching times were determined from the time elapsed between 90% and 10% transmissions. The results are summarized in Fig. 6. At high temperatures, both the relaxation τ_{off} and the

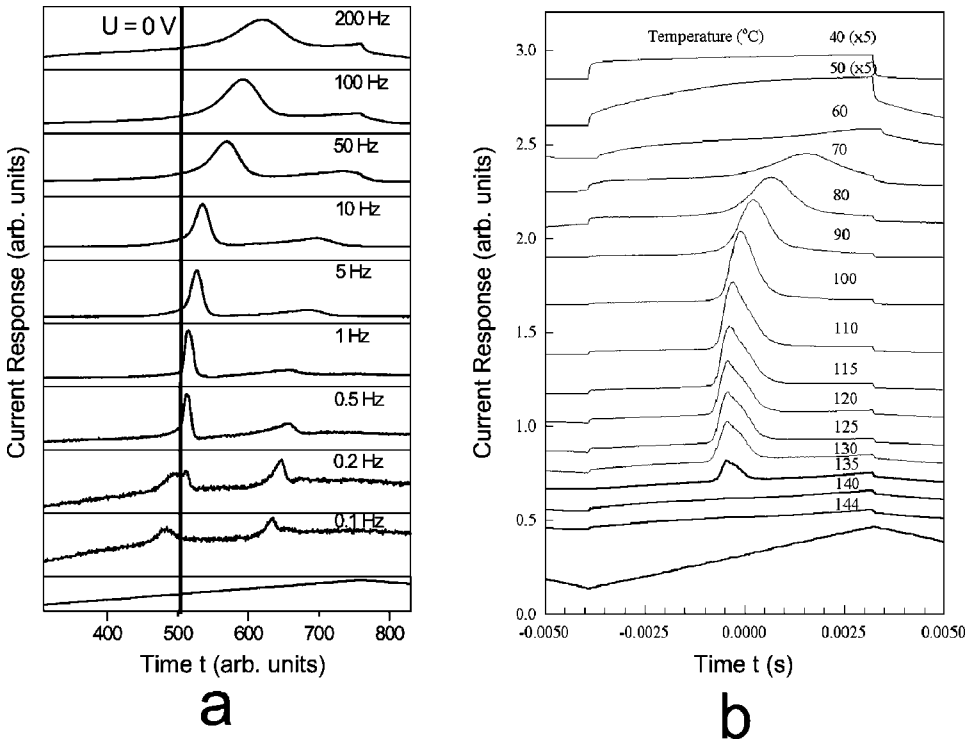

FIG. 5. Polarization current responses as a function of frequency at $T=100\,^{\circ}$C, $E=10\ \mathrm{V}/\mu$m, $d=10\ \mu$m (a); temperature dependence of the current response of a 4 μm cell (b). The amplitude of the triangular electric field is 20 V/μm, frequency is 70 Hz.

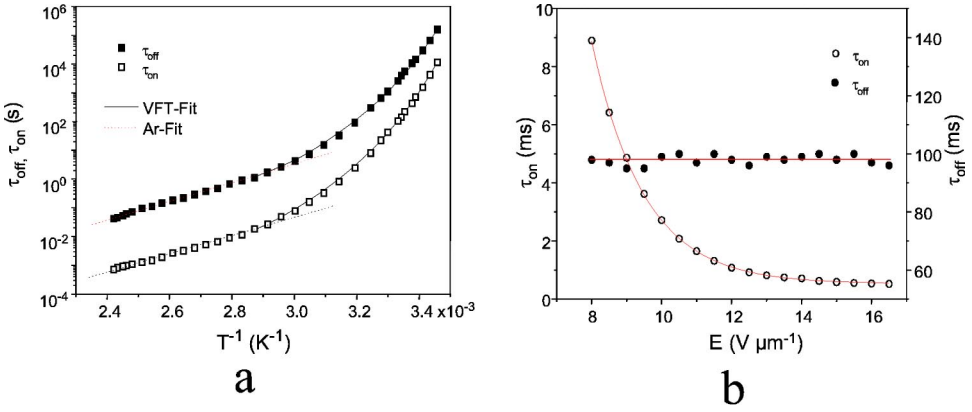

FIG. 6. (a) Temperature dependences of the switching times τ_{on}, and relaxation times τ_{off} as determined from the time dependence of the transmission of a 4 μm test cell when switched on, and after removing a bias field of $E=15\ \mathrm{V}/\mu\mathrm{m}$; lines represent fitting data to AR or VFT behavior. (b) Voltage dependences of τ_{on} and τ_{off} at $T=100\,^{\circ}\mathrm{C}$.

field-induced switching to the ferroelectric state τ_{on} can be described by assuming simple Arrhenius (AR) behavior: $\tau = A\exp(\Delta H/RT)$. Below $T=50\,^{\circ}\mathrm{C}$, however, both characteristic times can be described by the Vogel-Fulcher-Tamann (VFT) equation $\tau = A\exp[B/(T-T_0)]$, which is valid near the glass transition.

In Fig. 7 the dielectric loss ε'' of a 10 μm sample, measured with a Hewlett-Packard 4194 A impedance analyzer, is shown as a function of temperature and frequency. The relaxation below 1 MHz (mode 1) of the Sm-CP phase is attributed to the deformation of the antiferroelectric order of the molecules [8]. Additionally, at temperatures below 90 °C, a second mode (mode 2) occurred at higher frequencies. We think that it corresponds to a segmental reorientation, in particular, the reorientation of the terminal alkyloxy groups. Dynamic polarized Fourier-transform infrared studies will be done to clarify this proposal. We found that each relaxation process can be fitted by a separate Cole-Cole function. Additionally, at low frequencies the increase of ε'' due to ionic contributions was fitted by a power law $\varepsilon'' \sim \sigma/f^N$, where σ is the specific conductivity, f is the frequency of the measuring field, and N is an additional fit parameter. The relaxation times $\tau_r = 1/(2\pi f_r)$ are strongly temperature dependent. In the case of mode 1, the relaxation time ranges from 1 μs at $T=140\,^{\circ}\mathrm{C}$ to 0.4 ms at $T=50\,^{\circ}\mathrm{C}$. The dielectric strength of this mode has its maximum at $T=140\,^{\circ}\mathrm{C}$, where $\Delta\varepsilon=5.5$. This is a typical value for the achiral Sm-C_SP_A phase. The relaxation times obtained from both optical and dielectric measurements show reasonably good agreement (see Table I). One can see that the activation energy is of the order of $\Delta H \approx 62$ kJ/mol, except for mode 2. It is important to note that the temperature dependence of mode 2 can be described by a simple AR behavior, i.e., by a single exponential function. From the VFT fit to mode 1 we found that the Vogel temperature is $T_0 \approx -27\,^{\circ}\mathrm{C}$. This agrees with the theoretical prediction [14] that $T_g - T_0 = 30-50\,^{\circ}\mathrm{C}$, where T_g is the glass transition temperature. In the present case this means that $T_g = 3-23\,^{\circ}\mathrm{C}$, which is consistent with the differential scanning calorimetry results, which gave $T_g = 19$ and 14 °C in cooling and heating, respectively. Since we found that the polarization is not switchable below around 17 °C, we conclude that the rotations of the rigid cores of the molecules around the tilt cone are frozen below T_g, but the rotation of the terminal chain is probably still going on, as suggested by the Arrhenius behavior of mode 2.

It is very important that we were able to freeze both chiral and achiral states after applying suitable fields in the Sm-CP

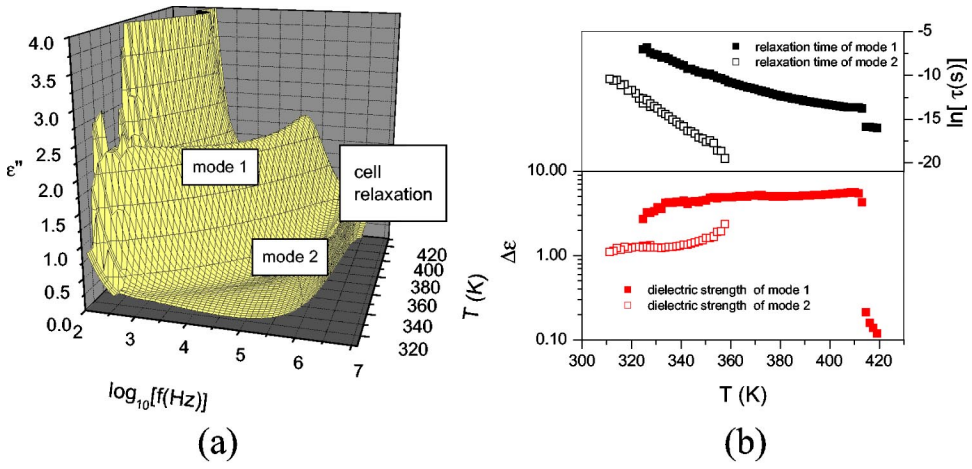

FIG. 7. Dielectric relaxation spectroscopy. (a) Dielectric loss ε'' as a function of temperature and frequency ($f_0 = 1$ Hz) of the applied field ($U = 0.1V_{rms}$) as measured in heating; the high frequency absorption is due to the resistance of the electrodes of the test cell ($d = 10\ \mu$m). (b) A fit to the data assuming separate Debye relaxation processes and an exponential function that allows for an increase of ε'' at low frequencies due to ions. The relaxation times and dielectric strengths of modes 1 and 2 are given as functions of temperature.

TABLE I. Characteristic times from electro-optic and dielectric measurements, and corresponding parameters determined from fitting the data to a VFT and an Arrhenius equation, respectively.

Characteristic time	ΔH (kJ mol^{-1})	A (s)	B (K)	T_0 (K)
τ_{on}	61.8	7.4×10^{-7}	1025	245.4
τ_{off}	62.4	1.3×10^{-4}	914	245.5
τ_{model1}	62.8	3.0×10^{-9}	1007	245.9
τ_{mode2}	175.0			

phase. As was mentioned above, the virgin samples were achiral; however, above 120 °C this could be transformed to the chiral state by applying $E=15$ V/μm, $f\approx1$ kHz bipolar square-wave fields. Under these conditions the liquid crystal showed a strong turbulent mechanical movement. On switching off the electric field from this state, a uniform texture formed that did not contain stripes within the individual fans. Interestingly, after $E_{dc}>2.8$ V/μm bias fields were applied and removed, the texture showed stripes, indicating that the dc field induced the achiral state again. As was described previously [10], three states (achiral antiferroelectric and chiral ferroelectric with + or − polarization direction) are opaque, whereas the other three states (chiral antiferroelectric and achiral ferroelectric with + or − polarization direction) are transparent. On cooling down the samples prepared in the above mentioned ways without applied voltages, both the chiral and achiral antiferroelectric states were frozen. On cooling under low frequency electric fields, both ferroelectric states could be frozen, and they did not transfer back to the antiferroelectric state even if the field was removed below T_g. The textures of these six vitrified states are shown in Fig. 8.

In order to clarify that the stored states indeed have different polar properties, we performed second harmonic generation (SHG) studies, since SHG signals require noncentrosymmetric arrangement of the molecules. Antiferroelectric Sm-CP banana-shaped smectic phases are apolar and show no SHG signal, whereas ferroelectric states of banana-shaped molecules generally show extremely high hyperpolarizability compared to other liquid crystalline or even crystalline materials [15]. The SHG activity above the glass transition temperature is plotted as the function of applied voltage in Fig. 9. The antiferroelectric nature of the sample is reflected by the double hysteresis loop: at zero electric fields the SHG activity is zero and sharply increases at $E_{th}\approx3.6$ V/μm ($T=40$ °C). After field removal the SHG signal relaxes to zero in times corresponding to τ_{off} obtained by transmission measurements (for example, at $T=20$ °C $\tau_{off}=200$ s), proving that both the SHG and the transmission measurements monitor the same ferroelectric-antiferroelectric relaxation mechanism.

Comparing the SHG signals of (R/S)-BiPhe with that of a Y-cut quartz crystal via the standard Maker fringe technique, the effective nonlinear coefficient of the sample was estimated to be $d_{eff}=1.1\times10^{-12}$ pC/N. This is twice larger than d_{11} of quartz, but is somewhat smaller than for other ferroelectric Sm-CP banana-shaped smectic phases [15].

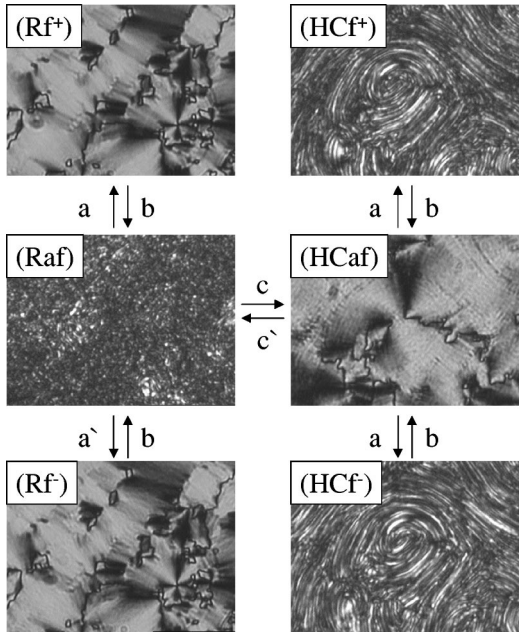

FIG. 8. Polarizing micrographs of a $d=10$ μm thick sample without applied voltages at 10 °C. The liquid crystal forms six states with either achiral (RAF, RF−, RF+) or chiral layer structure (HCAF, HCF+, HCF−); R indicates achiral and HC chiral states; AF and F denote the corresponding antiferroelectric and ferroelectric states. An interchange between the states takes place quickly when heating the sample to about 50 °C and applying the appropriate fields $E>|E_{th}|$ (a) and (a′), and at $E=0$ (b). The chirality of domains may be interchanged by heating the sample to 120 °C and applying either bipolar square electric fields of $f=1$ kHz and $E=15$ V/μm (c), or a triangular electric field $E=10$ V/μm and $f=100$ Hz (c).

Cooling the cell below the glass transition temperature during application of an electric field ($E=15$ V/μm), we found that the SHG signal is reduced by about 30%, which is comparable with other glass forming ferroelectric liquid crystals [16]. On switching off the field in the glassy state, the SHG activity did not relax, which means that the polar states are frozen. This offers the possibility of solid nonlinear optical (NLO) devices. On cooling the sample to the glassy state at zero field the SHG activity is zero.

III. DISCUSSION

A banana-shaped compound was synthesized possessing a polar liquid crystalline Sm-CP phase over a broad temperature range including room temperature. The tendency to form the crystalline state was reduced, first by introduction of a chlorine substituent in the central biphenyl core and second by use of a bulkier terminal chain (dihydrocitronellol). As a result no recrystallization occurred down to −50 °C. At room temperature the material has a high viscosity and the electro-optical switching is very slow. Thermal, electro-optical, and dielectric investigations all showed that the Sm-CP phase freezes into a glassy state below 17 °C, which cannot be switched by electric fields. Second harmonic generation studies gave evidence that the frozen states can be either polar or nonpolar. This behavior is useful in studying the

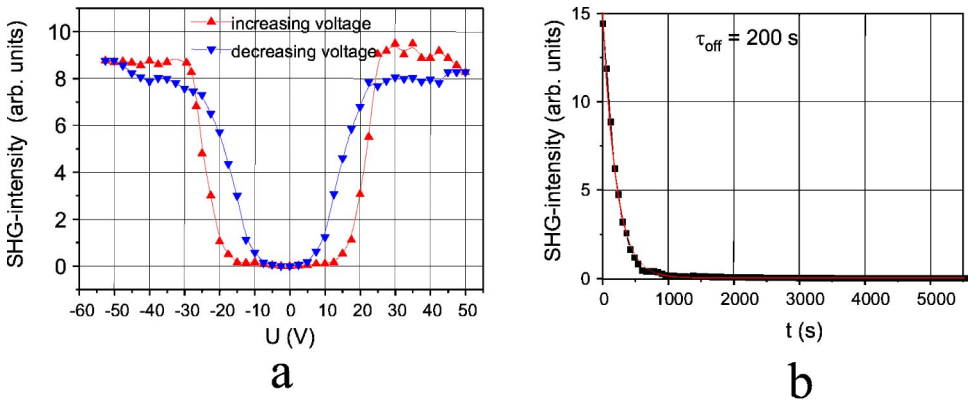

FIG. 9. (a) Voltage dependence of the *SHG*-activity of the achiral antiferroelectric state ($d=5\ \mu$m) with normal incidence of the fundamental wave measured with an *SHG*-microscope (spot size 30 μm) at $T=40\,^{\circ}$C, and (b) the *SHG* intensity after switching off the external electric field at $T=20\,^{\circ}$C. The fundamental wave is obtained from a *Q*-switched, chromium-doped yttrium-aluminum-garnet laser (Cr:YAG, $l0=1064$ nm)

different Sm-*CP* structures by surface imaging techniques, like atomic force microscopy. It also offers the possibility of designing nonlinear optical devices, for example, in optical waveguiding systems for efficient frequency conversion in poled structures. We can also envision electro-optical storage devices, where each of the optically distinguishable (opaque or transparent) elements can hide three additional electronic states (polarization $+$, $-$, or 0).

Finally, we discuss the appearance of a single polarization current peak, in spite of the fact that the SHG measurements clearly show that the phase is antiferroelectric. In addition, we explain why the polarization peak can appear in the decreasing part of the triangular form electric fields, i.e., why the switching to the opposite state happens before the sign of the applied external field changes.

Due to the presence of insulating layers and spontaneous polarization P_0, and ionic charges with surface density σ, the internal electric field E acting on a liquid crystal of thickness d will be different from the applied field V/d. It can be determined from the following equations [17]:

$$\varepsilon' E' - \varepsilon E = \sigma + P_0, \tag{1}$$

$$2\delta' E' + dE = V. \tag{2}$$

Here E', ε', and d' are the internal electric field, the dielectric constant, and the thickness of the insulating alignment layer, E, ε, and d are the corresponding values in the liquid crystal, and V is the applied voltage. From these equations we get that

$$E = \frac{V - 2d'/\varepsilon'}{d + 2d'(\varepsilon/\varepsilon')} \frac{\sigma + P_0}{\varepsilon}. \tag{3}$$

This shows that the internal field is negative even for positive potential, if

$$V \leqslant \frac{2d'/\varepsilon'}{\sigma + P_0}. \tag{4}$$

With $P_0 = 300$ nC/cm^2, $d' = 50$ nm, and $\varepsilon' = 3\times 10^{-11}$ we get that the field is negative below $V=10$ V. For a 4 μm cell this corresponds to a 2.5 V/μm field. If this field is larger than the threshold for switching, E_{th}, the polarization switches over before the applied voltage drops to zero. At lower temperatures, E_{th} increases, so the polarization peak appears only on the positive side, just as was observed experimentally [see Fig. 5(b)].

Since the dynamics of the ion motion is different from that of polarization switching, the presence of free ions results in another current peak. The magnitude and the position of this second peak depend on the charge density, mobility, and the activation field needed for ionization. The internal electric field and current were calculated based on Eq. (3), assuming both antiferroelectric and ferroelectric structures and an additional ionic flow with $\sigma = P_0/2$ (see Fig. 10). It is important to note that, even for antiferroelectric states, the polarization can be switched in one step if the relaxation to the antiferroelectric state is slower than the periodicity of the applied voltage. There is good agreement between the mea-

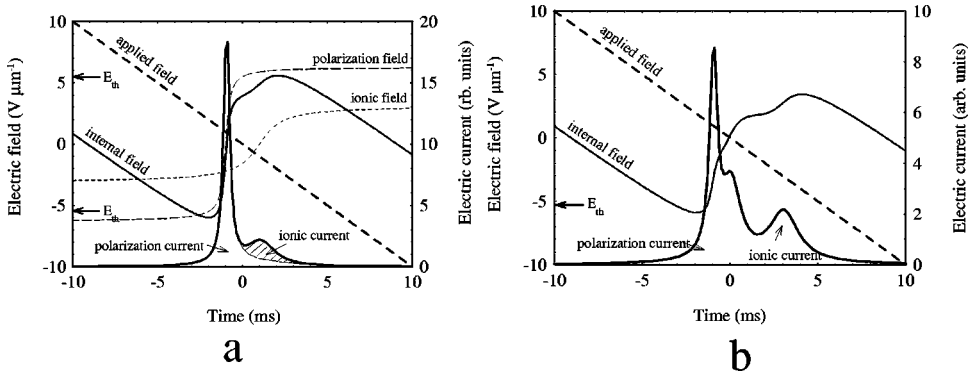

FIG. 10. Calculated time dependence of the internal electric fields and the polarization current due to triangular applied field: switching in (a) one step (ferroelectric state) (b) two steps (antiferroelectric state).

sured relaxation time τ_{off} and the period of the applied voltage where the peak of the positive slope disappears.

The slow relaxation from the ferroelectric state to the antiferroelectric one, and the observed glass transition instead of crystallization should have the same origin; possibly both are due to the presence of the bulky dihydrocitronellol terminal chain.

ACKNOWLEDGMENTS

This research was supported by the German Research Fund (DFG Project No. HE1167/11-2), the VolkswagenStiftung (Grant No. AZ: I/72875), and a Research Challenge Grant of the Ohio Board of Regents.

[1] T. Niori, T. Sekine, J. Watanabe, T. Furukawa, and H. Takezoe, J. Mater. Chem. **6**, 1231 (1996).

[2] D. R. Link, G. Natale, R. Shao, J. E. Maclennan, N. A. Clark, E. Körblova, and D. M. Walba, Science **278**, 1924 (1997).

[3] G. Pelzl, S. Diele, and W. Weissflog, Adv. Mater. (Weinheim, Ger.) **11**, 707 (1999).

[4] D. M. Walba, E. Körblova, R. Shao, J. E. Maclennan, D. R. Link, M. A. Glaser, and N. A. Clark, Science **288**, 2181 (2000).

[5] E. Gorecka, D. Pociecha, F. Araoka, D. R. Link, M. Nakata, J. Thisayukta, Y. Takanishi, K. Ishikawa, J. Watanabe, and H. Takezoe, Phys. Rev. E **62**, R4524 (2000).

[6] S. Rauch, P. Bault, H. Sawade, G. Heppke, G. G. Nair, and A. Jákli, Phys. Rev. E **66**, 021706 (2002).

[7] A. Jákli, Ch. Lischka, W. Weissflog, G. Pelzl, S. Rauch, and G. Heppke, Ferroelectrics **243**, 239 (2000).

[8] G. Heppke, A. Jákli, S. Rauch, and H. Sawade, Phys. Rev. E **60**, 5575 (1999).

[9] A. Jákli, W. Cao, Y. Huang, C. K. Lee, and L-C. Chien, Liq. Cryst. **28**, 1279 (2001).

[10] A. Jákli, D. Krüerke, H. Sawade, L-C. Chien, and G. Heppke, Liq. Cryst. **29**, 377 (2002).

[11] A. Hauser, H. Schmalfuss, and H. Kresse, Liq. Cryst. **27**, 629 (2000).

[12] Results will be published elsewhere.

[13] $1H$ NMR ($CDCl_3$, 300 MHz); $d=0.89$ $(6H,s)$, $d=0.91$ $(6H,s)$, $d=0.97$ $(3H,s)$, $d=0.99$ $(3H,s)$, $d=1.20$ $(6H,m)$, $d=1.36$ $(6H,m)$, $d=1.60$ $(6H,m)$, $d=1.88$ $(2H,m)$, $d=4.10$ $(4H,m)$, $d=6.97$ $(4H,dd)$, $d=7.34$ $(5H,m)$, $d=7.44$ $(1H,d)$, $d=7.66$ $(4H,m)$, $d=7.76$ $(1H,d)$, $d=8.07$ $(4H,dd)$, $d=8.34$ $(4H,dd)$, $d=8.61$ $(2H,s)$.

[14] A. Schönhals, F. Kremer, A. Hofmann, E. W. Fischer, and E. Schlosser, Phys. Rev. Lett. **70**, 3459 (1993).

[15] R. Macdonald, F. Kentischer, P. Warnick, and G. Heppke, Phys. Rev. Lett. **81**, 4408 (1998).

[16] M. Loddoch, G. Marowsky, H. Schmid, and G. Heppke, J. Phys. Chem. B **59**, 591 (1994).

[17] T. C. Chieu, K. H. Yang, Jpn. J. Appl. Phys., Part 1 **28**, 2240 (1989).